

VU Research Portal

Use of Satellite Information on Wetness and Temperature for Crop Yield Prediction and River Resource Planning

Basist, Alan; Dinar, A.; Blankespoor, B.; Bachiochi, David; Houba, Harold

published in

Climate Smart Agriculture
2018

DOI (link to publisher)

[10.1007/978-3-319-61194-5](https://doi.org/10.1007/978-3-319-61194-5)

document version

Publisher's PDF, also known as Version of record

document license

CC BY-NC-SA

[Link to publication in VU Research Portal](#)

citation for published version (APA)

Basist, A., Dinar, A., Blankespoor, B., Bachiochi, D., & Houba, H. (2018). Use of Satellite Information on Wetness and Temperature for Crop Yield Prediction and River Resource Planning. In L. Lipper, N. McCarthy, D. Zilberman, S. Asfaw, & G. Branca (Eds.), *Climate Smart Agriculture: Building Resilience to Climate Change* (pp. 77-104). (Natural Resource Management and Policy; Vol. 52). Springer. <https://doi.org/10.1007/978-3-319-61194-5>

General rights

Copyright and moral rights for the publications made accessible in the public portal are retained by the authors and/or other copyright owners and it is a condition of accessing publications that users recognise and abide by the legal requirements associated with these rights.

- Users may download and print one copy of any publication from the public portal for the purpose of private study or research.
- You may not further distribute the material or use it for any profit-making activity or commercial gain
- You may freely distribute the URL identifying the publication in the public portal ?

Take down policy

If you believe that this document breaches copyright please contact us providing details, and we will remove access to the work immediately and investigate your claim.

E-mail address:

vuresearchportal.ub@vu.nl

Use of Satellite Information on Wetness and Temperature for Crop Yield Prediction and River Resource Planning

Alan Basist, Ariel Dinar, Brian Blankespoor, David Bachiochi,
and Harold Houba

Abstract Satellite derived measurements are essential inputs to monitor water management and agricultural production for improving regional food security. Near real-time satellites observations can be used to mitigate the adverse impacts of extreme events and promote climate resilience. Population growth and demand of resources in developing countries will increase vulnerability in agriculture production and are likely to be exacerbated by the effects of climate change. This paper introduces wetness and temperature products as important factors in decision and policy making, especially in regions with sparse surface observations. These objective satellite data serve as: (1) an early detector of growing conditions and thus food supply; (2) an index for insurance programs (i.e. risk management) that can more quickly trigger release of catastrophic bonds to farmers to mitigate crop failure impact; (3) an important educational and informational tool in crop selection, resource management, and other adaptation or mitigation strategies; (4) an important tool in food aid and transport; (5) and management of water resource allocation. The two new indices (surface wetness and temperature) are meant to complement currently available datasets, such as the greenness index, soil moisture measurements, and river gauges.

A. Basist (✉) • D. Bachiochi
EyesOnEarth, Asheville, NC, USA
e-mail: alan@eyesonearth.org; dave.bachiochi@weatherpredict.com

A. Dinar
School of Public Policy, University of California Riverside, Riverside, CA, USA
e-mail: ariel.dinar@ucr.edu

B. Blankespoor
World Bank WeatherPredict Consulting, Washington, DC, USA
e-mail: bblankespoor@worldbank.org

H. Houba
Free University of Amsterdam, Amsterdam, Netherlands
e-mail: harold.houba@vu.nl

1 Introduction

As world population grows and income increases in developing countries, food consumption habits change, requiring more feedstock for animal production. Furthermore, climate change will have a direct impact on primary and secondary food production, caused by extreme temperatures, precipitation and river flow. This variability will have a direct impact on regional and global food and water supplies. To help vulnerable regions of the world cope with such challenges the concept of climate smart agriculture (CSA) directly addresses the need for adaptation in order to mitigate exposure to the hazards associated with interannual variability and climate change.

The information contained in this chapter demonstrates the value of satellite data (the wetness and temperature products) for monitoring crop production, food security, river flow, and river basin planning in many regions of the world. These products can serve as valuable climate smart decision-making tools in CSA. Specifically, there are several benefits to monitoring growing conditions from objective satellite derived observations:

1. They provide early warning to the available food supply, which mitigates the impact of reduced yields;
2. The wetness and temperature anomalies can be used as indexes in insurance programs as triggers in catastrophic bonds used to compensate the farmers for their losses in near real time;
3. The historic record of growing conditions can be used to identify the return period for various levels of crop failure, which can be used to define vulnerability and return periods for various levels of crop failure, which is essential information for risk management and premium calculation in the insurance industry;
4. Use of the climatology identifies the viability of alternative crop production, beyond the crops traditionally grown in the region. The production of multiple crops is a valuable hedge against catastrophic crop failure. Benefits may be complementary to mitigation activities, agricultural productivity, climate resiliency and natural resource management (Larson et al. 2015).

Since clouds at any one time covers over half of the world, clouds impact most of the surface signal of remotely sensed data across the world (Jackson 2005). Therefore, this study uses satellite derived microwave signals, since they penetrate through most cloud types. Consequently, they are effective in monitoring the surface through most sky conditions. In contrast, before infrared and visible signals can be used, they must be processed by sophisticated and complex cloud clearing algorithms, and can only effectively detect the surface under clear skies (Tucker et al. 2005). Moreover, the most interesting weather usually occurs under partly cloudy to overcast conditions. The microwave signal allows us to observe these events.

In an effort to derive surface temperature from microwave observations, it is necessary to overcome the primary source of noise in the satellite signal: water near the surface. Therefore we developed a technique to identify the magnitude of the

water and filter its influence (liquid water reduces emissivity in the microwave spectrum). Specifically, in order to detect land surface temperatures, this low temperature bias must be removed. In the process of accurately identifying the emissivity reduction associated with liquid water and removing its effect on reduction in temperature observations, we were able to accurately identify the magnitude of liquid water near the surface. This byproduct may be more relevant and useful than the surface temperature product we were attempting to observe. Therefore, this chapter will primarily focus on the utility of the surface wetness product and its applications. The wetness product detects: (1) Upper-level soil moisture; (2) Water accumulating into the drainage basins (rivers) of the world; (3) Melting snow packs; (4) Lakes and bogs; (5) Water in the canopy. Upper level soil moisture is effectively used to monitor agricultural yields and river discharge. Consequently, these measurements are essential to water resources management and food production.

There is a need for improvements in crop prediction models, both at high (field level) (Becker-Reshef et al. 2010) and moderate (district level) resolution (Deryng et al. 2011). The satellite-derived wetness index provides data at a moderate spatial resolution. It has been applied in the insurance industry for monitoring likelihood of crop failure throughout the world, and by various governmental and international organizations (e.g. United States, Canada, China, World Bank and UNDP) for assessing yield and food security around the globe, as well as to monitor flow discharge in rivers (e.g. Blankespoor et al. 2012). The goal is to expand the application to a larger client base and provide accurate yield predictions during the growing season. The product can also provide valuable information about adversity thresholds for various levels of crop failure, which is essential for determination of rates for crop insurance underwriting. Moreover, accurate near real monitoring program has several important benefits for CSA: (1) The prediction of yield directly impacts food security and activates infrastructure to move food from where it is in surplus to areas in need; (2) Knowing the wetness and temperature and how they impacts development of the various crops, can be used to optimize the crop types to field conditions, the information can be spread by agricultural extension agents; (3) Planting is one of the most important periods in crop production, it has been shown that the wetness and temperature can be used to optimize planting decisions.

Weather, climate, topography, and vegetation cover have the greatest impacts on the hydrology of a river basin and the variability of natural flow. However, human diversions on river discharge and the effects of climate change confound the predictability of water in the future (Jury and Vaux 2005; Miller and Yates 2006). Since changes in flow affect populations and society in profound social and economic ways, our lack of confidence in future water resources requires mitigations strategies to address the uncertainty (Palmer et al. 2008). Specifically, hydrologic variability creates a significant challenge to countries, since high or low flow events may lead to flooding damage, severe drought, destruction of infrastructure, and/or fatalities. These events promote economic shocks and even generate intra-state violent conflict (Drury and Olson 1998; Nel and Righarts 2008; Hendrix and Salehyan 2012). Moreover, water variability affects international political tensions (Adger et al. 2005; Intelligence Community Assessment 2012). This may even occur in

basins where mitigating institutions (like water treaties) have been negotiated (Drieschova et al. 2008). In other words, uncertainty and lack of predictability in flow increases tensions between sectors within a society, as well as between riparian states (Ambec et al. 2013), and the availability of water resources is central to CSA in many areas of the world.

The importance of having a good estimate of the water supply is the foundation of allocation and distribution of irrigation supplies. Since the wetness index is highly sensitive to liquid water near the surface, it effectively quantifies the melting snowpack, and this water feeds many irrigation supplies around the world. Since the origin of the water is monitored, there is a valuable lead-time to communicate with decision makers and allocate the water based on CSA principals and guidelines.

Lakes and bogs are generally permanent features observed by the wetness index, although they may slowly change in size. Since they are a significant component of the surface wetness signal, it is useful to remove these permanent features from the variable signal observed by the index: specifically, water on the upper section of the soil and held in the canopy. Since water in the canopy has an association with leaf area, part of the signal represents the health of the crop. Our goal is to filter the permanent features, the climatology, and the annual cycles, and focus on the inter-annual variability in wetness, which is driven by the weather. Anomalies are the best tool to achieve this goal. Therefore, the crop models are based on anomalies.

The wetness product is hereafter noted as the Basist Wetness Index (BWI), which detects water near the surface from multiple sources (as mentioned above). In order to simplify the interpretation of the BWI, it is calculated as the percentage of the radiating surface that is liquid water. A reasonable spectrum of this value would be zero percent in desert regions, while agricultural areas have values ranging between 2 and 10% of the surface that is liquid water. Values above 10 usually indicate a very wet surface, such as recently melted snow cover or recent rain.

The following section presents the methodology used to define the BWI, and as well as how it can be used to estimate present and future water supplies under situations where traditional (surface based) observations of surface water are not available, as is the case in many countries. Section 3 illustrates the use of these satellite driven monitoring tools in three different applications (predicting yield of agricultural crops, estimating river flow, and planning in a river basin). The chapter discusses several other applications without demonstrating them, for space consideration.

2 Methodology

The BWI index is derived from a linear relationship between channel measurements (Eq. 1), where a channel measurement is the value observed at a particular frequency and polarization, i.e. the Special Sensor Microwave Imager (SSM/I) observes seven channels (Basist et al. 1998).

$$BWI = \Delta\epsilon \cdot T_s = \beta_0 [T_b(v_2) - T_b(v_1)] + \beta_1 [T_b(v_3) - T_b(v_2)] \quad (1)$$

where the BWI is the percentage of the surface that is liquid water (Basist et al. 2001), $\Delta\epsilon$, is empirically determined from global SSM/I measurements, T_s is surface temperature from station measurements, T_b is the satellite brightness temperature at a particular frequency (GHz), ν_n ($n = 1, 2, 3$) is a frequency observed by the SSM/I instrument, β_0 and β_1 are estimated coefficients that correlate the relationship of the various channel measurements with observed in situ surface temperature at the time of the satellite overpass. Specifically, as wetness values increase, the differences between the observed surface temperature and the observed channel measurements also increase (Williams et al. 2000).

Weekly and monthly average BWI values are very good indicators of the magnitude of water near the surface, which has a relationship to water at greater depths. These observations have proven valuable in agricultural monitoring during the previous 25 years of analytical work. The wetness anomalies have proven valuable in predicting agricultural yields in many areas of the world (Curt Reynold USDA, personal correspondence). Research indicates the wetness product has a gamma distribution, much like precipitation (Gutman 1999); therefore a gamma distribution is used to derive the variation of wetness from the expected value.

Since most regions of the world have annual cycles associated with their liquid water near the surface, it is best to calculate anomalies for each pixel, location and time of year. The resolution of the pixel is 33 km by 33 km, and anomalies are calculated on a monthly and weekly basis. A value of 0.01 means that only 1 year in a 100 would realize a value so low (extremely dry) at the location for a particular time of year. Conversely, a value of 0.99 corresponds with an excessively wet event that only occurs one out of a 100 years. In summary, values progressively less than 0.5 indicate increasingly drier conditions and values progressively greater than 0.5 indicate increasingly wetter conditions than the expected value (Fig. 1).

The period of record for these wetness and temperature products begins in 1988 and they have been maintained in near real time for decades.¹ There is a period of 2 years, 1990 and 1991, when the stability of the microwave satellite instrument was deemed unreliable. Therefore, these 2 years are removed from the analysis. The climatology we use is based on the 23 years of data from 1988 to 2010. A series of operational satellite instruments flown by the United States Meteorological Satellite Service comprise the period of observations. Great effort has been made to seam the observations between the various satellite instruments into one contiguous record. A daily set of observations is composed of 14 orbits across the globe. These observations are sun synchronous over the equator, at an overpass time around 6 a.m. and 6 p.m. every day. The morning and afternoon overpasses are processed independently and then combined together into one set of observations across the globe. Each set of observations is added to this record in near real-time, as both weekly and monthly fields of temperature and wetness values.

¹ SSMI based temperature and wetness data and algorithms discussed in this chapter are a proprietary technology owned by WeatherPredict Consulting, Inc.

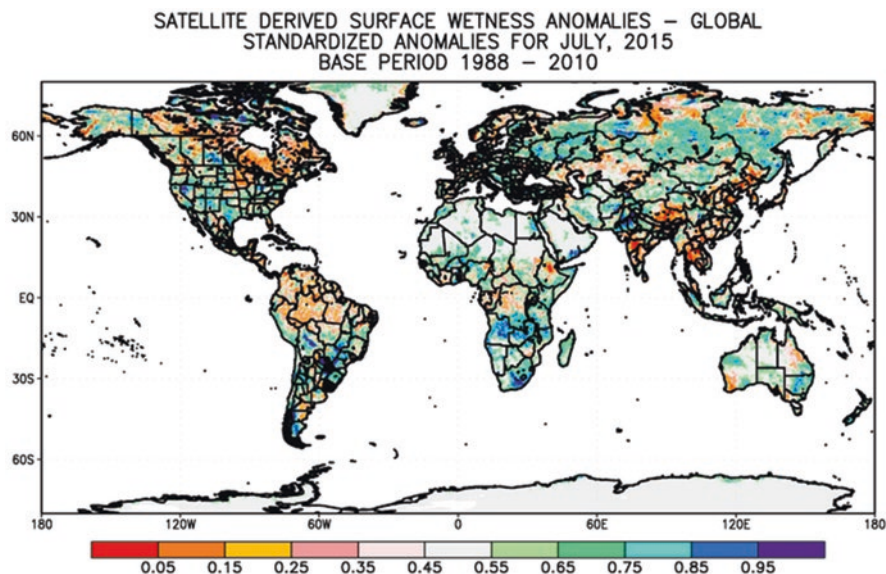


Fig. 1 Global surface wetness anomalies for July 2015. Note: The *grey* shade of the legend corresponds with the expected value, while values to the *left (right)* of the *grey* shade correspond with increasingly drier (wetter) than average conditions. For example, the value of 0.05 means that only 5% of the time is it that dry at a location and time of year. Inversely, a value of 0.95 means that only 5% of the time is it that wet at a location and time of the year

The actual wetness observations (not the anomaly) are valuable for measuring river discharge. These values identify the percentage of the radiating surface that is liquid water. Moreover, in many river basins there is 1–2 months lag in the time it takes for water in the upper section of the watershed to pass a monitoring gauge in the lower section of a river basin (where most people live and economic activity takes place). This lag, which averages prior month(s) BWI with the concurrent month (hereafter noted as the cumulative lag) improves the skill of the model to predict the flow passing through a river gauge. It also provides valuable lead-time to predict and mitigate the magnitude of drought or flood heading into the lower basin, where the impacts are generally most severe. Therefore, the early warning can be used to mitigate the impact of extreme events on society. An added advantage of applying a quantitative flow model, which can predict flow downstream, is that a consortium of riparian states can use the information to determine how the water resources will be distributed under various flow regimes. Therefore, treaties have the capacity to allocate water as a function of an independent and quantitative measure of flow, providing a simple and accurate predictive model for a fair and transparent distribution of water under times of scarcity.

The observations of the BWI spanning national borders allows for an objective (independent of national influence) calculation of water resources under almost all sky conditions. Since the wetness index is an independent tool that integrates the

accumulation of water across large areas, it has the potential to be used as an index and/or trigger for: (1) implementation or call to action in mitigation strategies; (2) insurance compensation; (3) allocation of water between sectors of society; (4) distribution of water between riparian states. These are important applications that warrant further research.

The following section demonstrates the use of the BWI tool for: monitoring crop yield, monitoring river flow, and river basin management. The Mekong River is used as an example. While these applications are site specific, the extrapolation from one site to another is easily done and can be accomplished with minimal cost to the agency.

3 Application

Currently, the wetness and temperature anomalies have proven valuable for monitoring crop development and assessing potential yields during the growing season, and have been effectively applied in crop yield prediction models. These models are statistically-based, using linear relationships between the wetness and temperature anomalies and yield, which serves as the calibration. The statistically-derived model parameters are used to predict yield during real time growing conditions and have been applied by many organizations around the world to assess future yields, as well as support planning policies related to the regional, national and global food security (Fig. 2).

There are several limitations in applying the wetness and temperature anomalies across various regions of the world. The first is the large footprint ($33 \text{ km} \times 33 \text{ km}$), which is about 1000 km^2 . This limits the application into a mesoscale analysis and has limited value for high-resolution assessments. Another limitation is coastal boundaries. Specifically, locations within 30 km of a coastline (ocean or large inland water bodies) will unduly influence the temperature and wetness products, since the presence of more than 50% water destabilizes the model, requiring that those signals be recognized and removed from the data sets. Exposed soils or rocks (dry areas) where minerals are exposed on the surface, introduces noise in the signal. This is particularly true when limestone is exposed on the surface. In these instances the product should be used with caution.

3.1 *Monitoring Crop Yield*

The yield prediction models are uniquely calibrated for each crop and particular locations. Specifically, yield prediction models are calibrated on historical values, using the linear variations of temperature and wetness anomalies as predictors. In addition, the quadratic of the wetness and temperature interaction is a predictor in the model. The models are run as the crop enters the reproductive stage, and

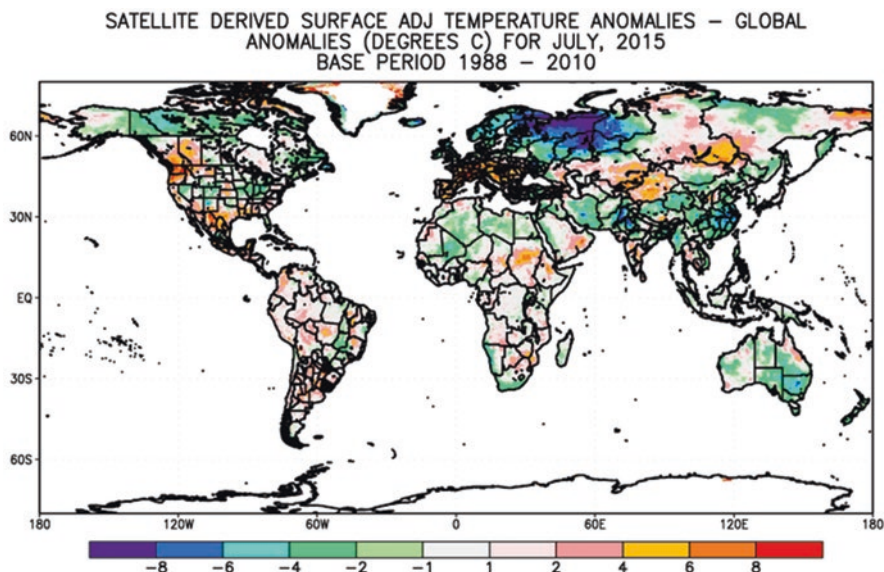


Fig. 2 Global surface temperature anomalies for July 2015. Note: The grey shade in the legend corresponds with the expected value, while values to the left (right) of the grey shade correspond with increasing colder (warmer) than average values. For example the value of -8 means that temperatures were -8°C colder than average at the location and time of year. Inversely, a value of 8 means that it was 8°C warmer than average at a location and time of the year

continues to be updated on a monthly basis through the maturation stage of the crop. The most important month of the growing season is usually reproduction, and therefore the influence of this period has a strong relationship to yield. The benefit of the interactive term is multifold. Specifically, linear statistical models tend to be mean-centric, which means they are challenged to capture extreme events. The quadratic component of their interaction generally captures these extreme events in the model.

The models are generally run at the district level. Moreover, each country is unique in the way that it reports yield data. The spatial resolution of the yield data provided by a country serves as the basis of calibration in the model. Both deviation from expected yield and actual yield prediction are presented in the findings of the report. The expected yield has been trended to account for linear improvement of seed stock and improved agricultural practices. These trends are removed, since they are independent of the weather. An example report on the corn belt of the USA during the 2015 growing season is presented below.

Figure 3a shows the predicted deviation from trended (expected) corn yields for the center of the corn-belt in the United States at the end of August 2015. The reasons this region is chosen are twofold; it produces one of the highest yields and is one of the most important growing areas for corn in the world and the sophisticated procedure for calculating yield by the United States Department of Agriculture (USDA) provides one of the best data sets for calibrating the yield prediction

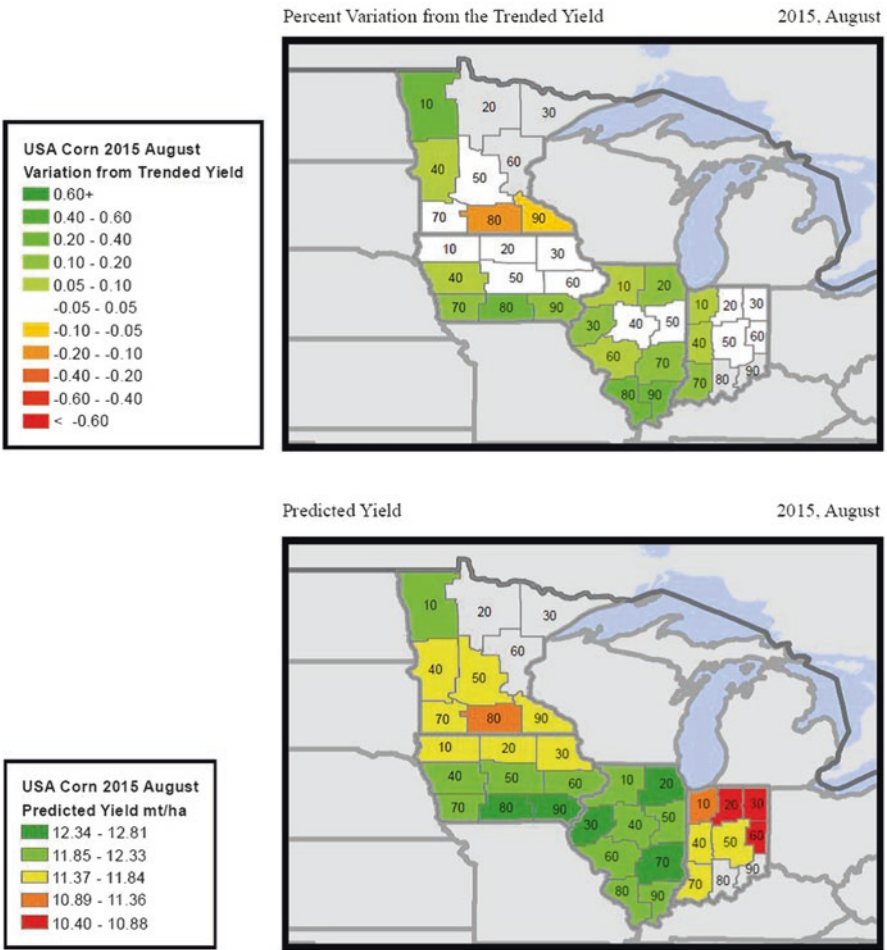


Fig. 3 (a) The percentage departure from the expected (trended) yield. (b) The predicted yield in Mt/ha. Note: Zero departures are *white*, and the departures are more amplified the color gets darker towards *red* (*below*) expected, or *green* (*above*) expected yields. They are displayed percentages from the expected value

models. August was chosen, as it provides an early warning to projected yield, as the crop has already entered seed-pod filling.

Generally, the predictions in this report range from average to above average yields for the primary growing regions in the United States. The exceptions are in southeastern Minnesota, where predictions are generally below the expected value. Yields, which have the greatest deviation above the expected values, include much of Illinois and southern Iowa. These areas had near average wetness and slightly below average temperatures, thereby promoting healthy growing conditions during the corn's development. The cooler than average temperatures allowed many areas with some moisture deficit to achieve near average yields, since the cool temperatures limited the moisture stress in the crop. Figure 3b displays the predicted yield as metric tons per hectare. The area with the highest yields occurs in locations where corn tends to produce some of the best yields in the world, and these areas also had better than average growing conditions. Note that the low yields in northern Indiana (where yields are near the expected value) indicate that growing conditions are generally inferior, compared to some the neighboring crop districts.

Figure 4 shows the wetness and temperature anomalies, which are used to predict corn yields for the center of the USA growing area. Predictions include data from May, June, July, August, the plot in fig. 4 displays the anomalies for July, which is the most important period in the determination of the yield. August is the time when seed pod filling occurs, after reproduction, it is the most critical period in the development of corn yield.

The above-average temperatures in July across areas of Iowa and most of Minnesota introduce heat stress, which reduces potential yield. Fortunately, there was ample moisture across most of the area, so the negative impact of excessive heat is nominal, in terms of yield reduction. More soil moisture is available in portions of Indiana and Illinois, and these areas are the regions with better than expected yields.

The parameters of the predictive model along with its calculation of yield are presented in Table 1. These values are presented by crop district for the state of Iowa. The location was chosen since it is the most important agricultural state for the production of corn. The slope for the trend of corn yields over the period of record is 0.16 (shared across the state), which means that the average annual increase in yield, due to improved seed stock and agricultural practices is 0.16 metric tons/ha/yr. The intercept for each crop district is unique, since some crop districts produce higher yields than others. The predicted yield is the model derived yield, in metric tons per hectare, for each crop district, based upon its wetness and temperature anomalies throughout the growing season to August 2015. The trended (expected) yield value is based on the 2015 crop season. The last column on the right is the percent variation from the expected yield, the parentheses means the value is negative.

Figure 5 illustrates that some crop districts are slightly below the expected value in terms of yield. However, the majority of the crop districts had higher than expected yield. Therefore, at the end of August the state of Iowa as a whole is predicted to have higher than expected yield. At this time of the growing season the seedpods are approaching maturity, and they provide a reliable measurement of the final yield.

The regression equation and statistical significance of each predictor variable in the model are presented in Table 2. The adjusted R^2 for the model is 0.60 with an F-statistic of 28.46. The model has 211 degrees of freedom. The predictive variables

8/26/2015

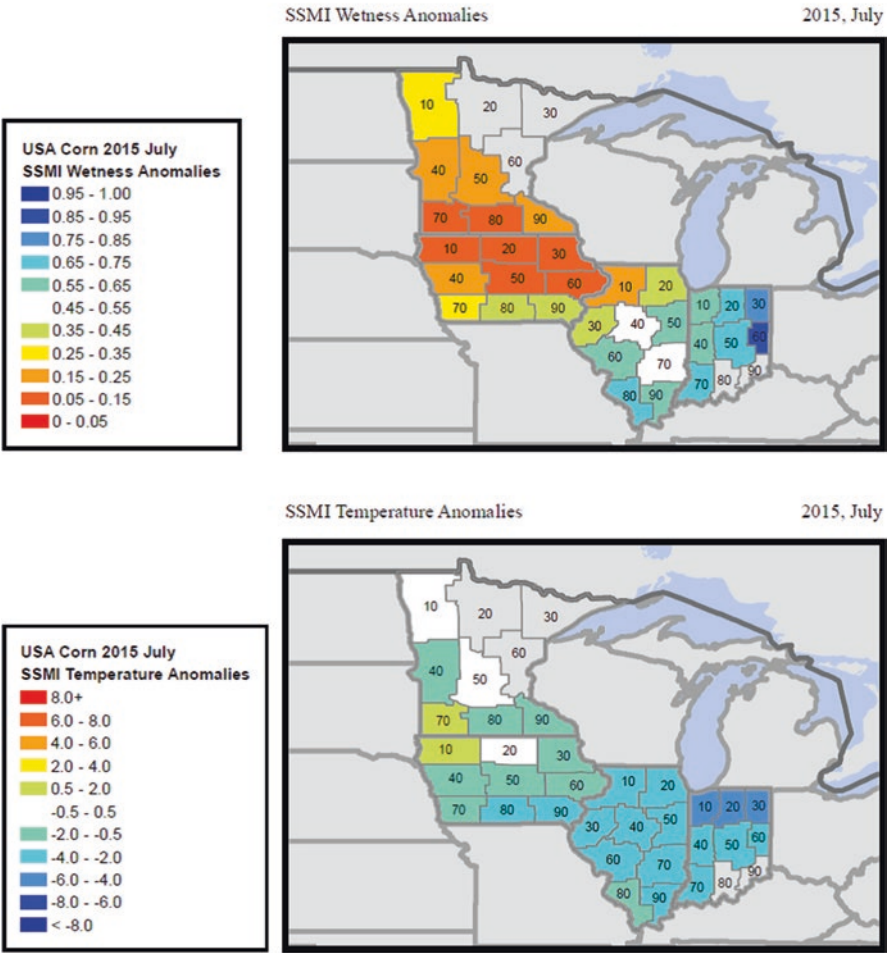


Fig. 4 July values are presented by crop districts: (a) Surface wetness anomalies are displayed by color, where shades towards *blue* (*red*) are increasingly *above* (*below*) the expected surface wetness value (see text for more details). (b) Surface temperature anomalies are displayed by color, where shades towards *blue* (*red*) are increasingly *below* (*above*) the expected surface temperature

are temperature and wetness anomalies from May, June, July and August. Also, the interaction of temperature and wetness is included as an independent variable in the model. The negative coefficients are portrayed in red and are inside parentheses. Predictive variables that are significant at the 0.90 confidence level are checked in the right-hand column. The most important variables in the model are the interaction of temperature and wetness in June and July, and the temperature in August. These three variables are all significant above the 99 percent confident interval.²

²The interactions of temperature and wetness for June and July are two of the strongest predictor variables in the model.

Table 1 Regression-model derived parameters for Iowa

Corn						
United States, Iowa						
Percent variation from trended yield						
Crop districts, ASDS based						
SSMI collection data date 8/26/2015						
	GeoID	Slope	Intercept	Pred yield	Trend yield	
Admin region	Crop district	mt/ha	mt/ha	mt/ha	mt/ha	Percent variation from trended
Buena Vista	19_10	0.16	7.53	11.45	12.05	(0.05)
Butler	19_20	0.16	7.46	11.48	11.98	(0.04)
Allamakee	19_30	0.16	7.26	11.53	11.78	(0.02)
Audubon	19_40	0.16	7.10	12.27	11.62	0.06
Boone	19_50	0.16	7.51	12.19	12.03	0.01
Benton	19_60	0.16	7.22	12.29	11.75	0.05
Adair	19_70	0.16	6.54	12.28	11.06	0.11
Appanoose	19_80	0.16	5.69	12.81	10.21	0.25
Davis	19_90	0.16	6.45	12.74	10.97	0.16

Identifies the slope and intercept for the linear trend in yield derived by the USDA yield values from 1988 to 2014

Note: The three columns to the right are predicted yield derived from the wetness and temperature anomalies, trended (expected) yield, and the column on the right is the ratio of the predicted/ trended yield for August 2015 (parenthesis means the values are negative).

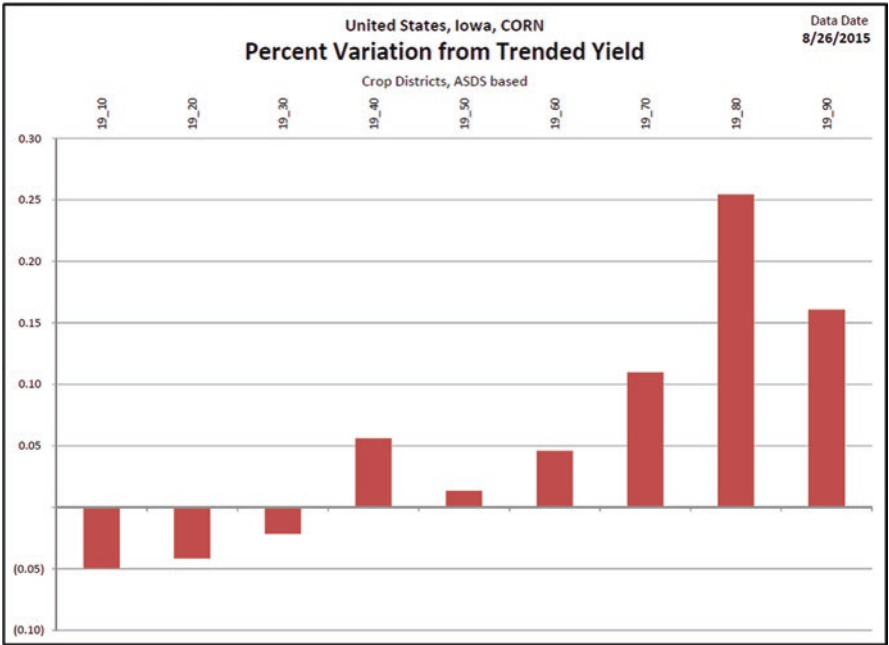


Fig. 5 Graphical representation of the variation from trended yield, in Iowa plot is conveyed by crop district in the state

Table 2 Model coefficients and significance values

Corn			
United States, Iowa			
Statistical model output			
Crop districts, ASDS based			
Data date 8/26/2015			
# observations	225	R-squared	0.62
# variables	13	Adjusted R-squared	0.60
Degrees of freedom	211	F-Statistic	28.46
Variables	Coefficients() negative values	Significance (in percent probability)	Significance @ 90% confidence
Constant	13.28	0.00	×
Temp May	0.05	0.01	×
Temp Jun	0.01	0.69	
Temp Jul	(0.05)	0.03	×
Temp Aug	(0.17)	0.00	×
Wet May	(0.19)	0.58	
Wet Jun	(1.06)	0.00	×
Wet Jul	(0.57)	0.24	
Wet Aug	0.11	0.78	
Interact May	(0.00)	0.10	
Interact Jun	(0.02)	0.00	×
Interact Jul	(0.02)	0.00	×
Interact Aug	(0.01)	0.10	

The degrees of freedom in the model, along with its predictive skill, regression coefficients, their significance level for each predictor variable Negative coefficients are in parenthesis

Finally, a scatterplot of the wetness and temperature anomalies for the months of July and August at the crop district level is presented (Fig. 6). Note that in the month of July the majority of Iowa had slightly below normal temperatures, while wetness values were drier than normal during the month. The lack of heat stress during reproduction was for yields. August continued to bring drier than average conditions to the majority of the state, while near average temperatures helped minimize soil moisture stress. Therefore yields predictions were near-normal. The forecast generally remained the same between the end of July and the end of August, since July is the most important month for yield prediction. Although there were changes in field conditions across a few crops districts during the August, the additional information in August improves the model skill as the crop reached maturity.

3.2 *Monitoring River Flow*

Quantitative and indepenedent measurements of river flow levels are essential for water rights and planned allocations. Moreover, reliable and independent measurements of available water resources are required for mitigation strategies and

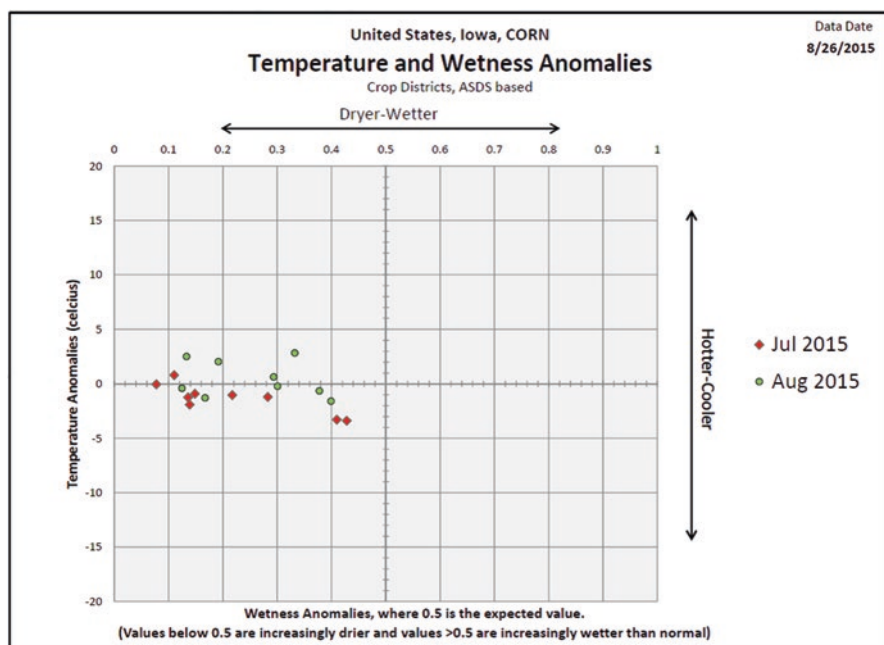


Fig. 6 Scatter plot of wetness and temperature anomalies by crop district for the months of July and August. Note: *Top left* quadrant is above temperature and below wetness, *bottom left* is below both temperature and wetness, *top right* is above both temperature and wetness, and *bottom right* is below temperature and above wetness

insurance compensation, which are a fundamental component of an effective treaty (Dinar et al. 2010) that allows proper planning and allocation of the basin water to various water consuming activities. Also, independent monitoring of flow measurements is required to implement an effective treaty, which is based on triggers, response and compensation, or to operate reservoirs used for irrigation projects. Therefore, high quality flow data are a necessary component of effective treaty stipulations and institutional mechanisms (Dinar et al. 2015), as well as infrastructure for reservoirs that can deal with future challenges. Real time data can also provide policy makers and researchers with the ability to predict extreme weather events, and cooperatively address economic impacts on existing projects. In addition, models can increase institutional capacity by providing timely (near real time) flow information to build climate resilience and effective sharing and allocation of limited water resources.

Considering the challenges to estimate flow where standard measurements are not available, we demonstrate a simple, yet robust model to predict both present and future flow measurements, using the wetness product in two basins: Zambezi and Mekong. The period of record for calibration of the models is from historic river gauge values, and these flow values are regressed on the BWI values (the predictor of

flow). In order to keep the equation as simple as possible, yet robust, the regression is based on one variable and tested in two basins of very different climatology's, topography's, land use patterns and annual water supply cycles. An important consideration between the gauge and BWI values is a lagged relationship between water accumulating near the surface and detected downstream at the gauge. The lag between the water input upstream and the detection of changes in flow downstream is based on numerous empirical observations and theory that flow models are more accurate when they include the prior month(s) due to the time lapse for the water accumulate into the major stem of the river (Demirel et al. 2013). The number of prior months used in the predictions of flows is directly related to the size of the basin, the influence of snow melt and its topography. Therefore, a lagged term is included in Equation 2, where $Q_{m(BWI)}$ is the discharge at a station for month m While n is the number of previous month(s) averaged together with the concurrent month BWI value.

$$Q_{m(BWI)} = g(d)$$

(2)

where $d = \frac{\sum_{i=0}^n BWI_{m-n}}{n}$.

Table 3 lists model statistics and parameters for the two river basins. The number of month(s) lagged prior to the gauge observations is included, along with the parameters of the regression model. Our goal is to define a simple and robust prediction from one variable and explore the utility of the predictor in areas of society that could benefit from the models.

The Zambezi model flow signature is clearly curved (Fig. 7a); it has a quadratic structure of high wetness values and extremely high flow. High values display considerable heteroscedasticity (from the studentized Breusch-Pagan test), which implies that numerous factors impact the high rate of flow past the gauge. In contrast, low BWI values (less than 1) contain a high confidence that the flow will be near the base flow. These results compared favorably to model prediction for the Zambezi presented by Winsemius et al. (2006), whose predictions were based on a more complex model. As a result, the BWI can be a quantitative indicator for periods and frequencies of flow associated with limited water – of particular relevance to obligations and commitments agreed upon in international water treaties.

Table 3 Parameters from Zambezi, Mekong predictive river flow models

Model	Zambezi (BWI)	Zambezi (precip)	Mekong (BWI)	Mekong (precip)
Linear term	−420.2	71.9	303.8	75.9
Quadratic term	748.6	0.78	886.6	0.297
Months lagged	2	2	2	2
month observation	148	198	44	44
Predictive skill (R2)	0.89	0.52	0.95	0.97
Residuals	485	1020	645	523

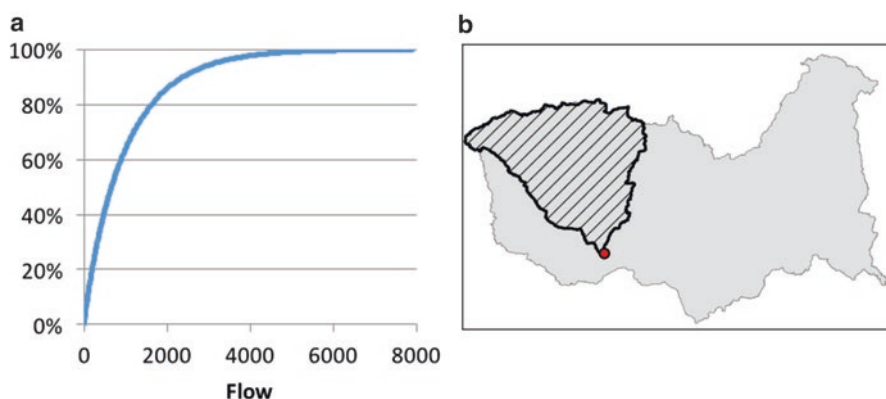


Fig. 7 (a) Cumulative distribution of flow using a gamma distribution (percent. y-axis) and flow (m^3/s per month. x-axis) of the Zambezi river basin sample area; (b) Map of Zambezi basin (grey) with the selected gauge data (point), international border (line) and respective catchment (hatched) used in the model

The lower bound of predicted flow is $288 \text{ m}^3/\text{s}$ ($\text{BWI} = 1.0$) occurs approximately 28% of the time. Therefore, for the Zambezi River at the Katima Mulilo station, approximately 28% of the time the flow is less than $288 \text{ m}^3/\text{s}$ averaged over the 3 months. The area feeding water to the gauge is defined in Fig. 7b.

Since the SSM/I instrument is currently operational, it is possible to use the fitted model to predict recent runoff from monthly wetness values, based on the calibration period. Due to the accuracy and significance of the models, we chose to explore the ability of the BWI to predict seasonality, low flow (e.g. droughts), and high flow events (e.g. floods). This analysis was used to explore the utility of the model in *serving as an early warning indicator*.

With regards to the Zambezi, the BWI model identified and predicted a flood in 2010, which according to the model is higher than any previous flood over the period of the SSMI record (Fig. 8). In April 2010, there is a pattern of large positive surface wetness anomalies in Western Zambia (Fig. 9). This broad pattern of purple indicates that the area was extremely wet conditions. This extreme event occurred across a large section of the basin. In rare instances, when there is an extreme flood on the Zambezi, due to heavy rainfall on the highlands in Angola and Zambia, the flow can actually accumulate at the Mambova fault. During this instance, the river expands over the flat floodplain behind the fault until the waters meet the channel cut by the Chobe River in the south. During this extreme flood, the accumulation of water from the Zambezi River overcomes the Chobe River, and water begins to flow upstream on the Chobe, flowing into Lake Liambezi. At the height of the flood, water flowed directly into Lake Liambezi from the Zambezi River through the Bukalo Channel on May 8, 2010 (NASA 2010), which is the same time the BWI predicted the highest flow over the period of record.

Next is discussed the Mekong model, which is presented in Table 3. The section of the river basin that feeds the Mekong gauge station is presented in Fig. 10b. The best explanatory model has a non-linear relation. The Mekong models also used a

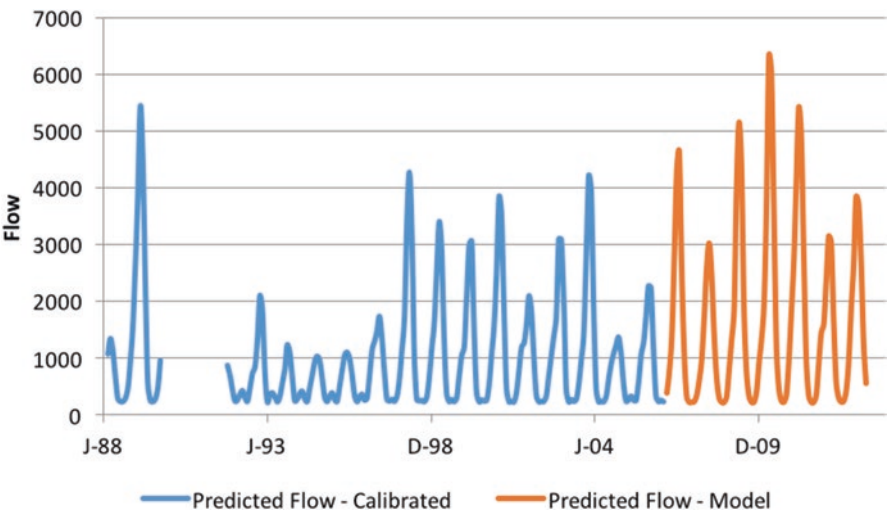


Fig. 8 The Zambezi values of runoff (m^3/s per month, y-axis) and time (x-axis, January 1988 through July 2013). The time series displays seasonality and interannual variability over the predicted (calibration) period in red (*blue*). The highest flow occurred in April/May 2010. Missing values are due to the lack of reliable SSM/I data

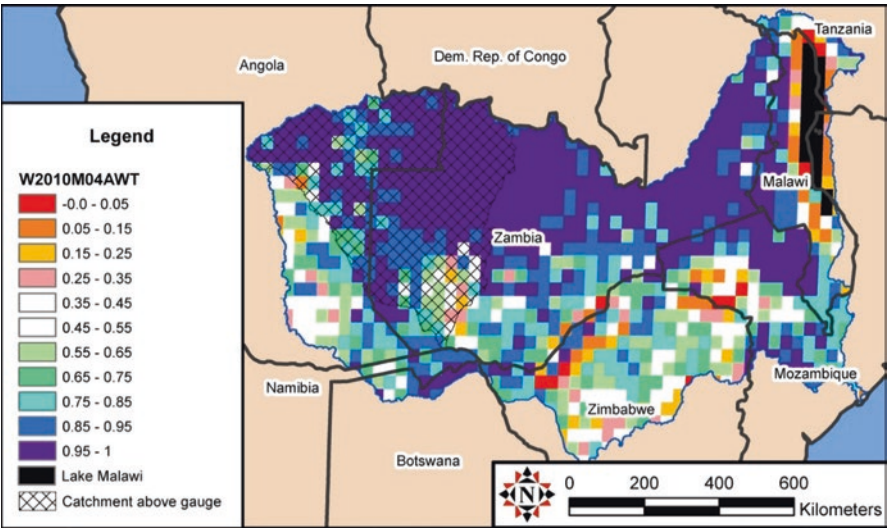


Fig. 9 Surface wetness Values for a section of the Zambezi River: April 2010, where 0.00–0.05 (*red*) means that less than 5% of the time is it this dry, 0.45–0.55 (*white*) is the expected normal soil moisture, and 0.95–1.0 (*purple*) means less than 5% of the time is it this wet

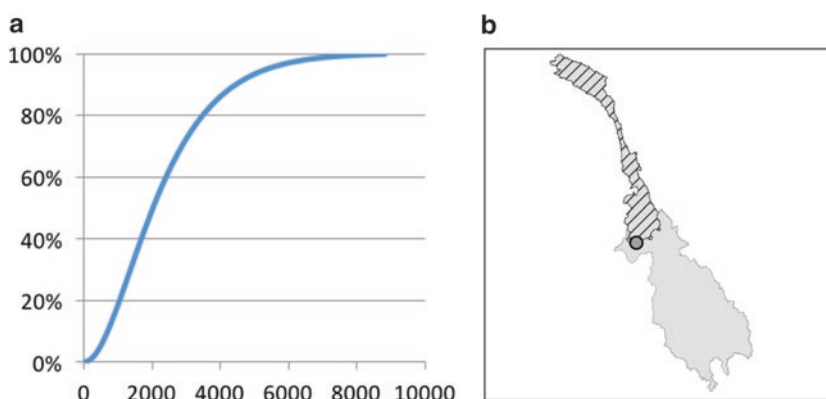


Fig. 10 (a) Cumulative distribution of flow using a gamma distribution (percent. y-axis) and flow (m^3/s per month. x-axis) of the Mekong river basin sample area. (b) Map of Mekong basin (grey) with the selected gauge data (point) and respective catchment (hatched)

quadratic form. It also implies that predicted flow below $1215 \text{ m}^3/\text{s}$ ($\text{BWI} = 1.0$) occurs less than 25% of the time. There is a limited period of calibration data, and some concern about the accuracy of the model. Therefore, an evaluation of the skill during the predictive period will demonstrate the robustness of this approach to monitor flow from the BWI data.

The Mekong river model captures the seasonal hydrologic variation (Fig. 11). The peak flows typically happen in September (end of the monsoon season), while typical low flow is in February. The calibration period ended in 1993, while the model predicted extremely high flow in September of 1995. We evaluated the accuracy of this predictions with meta data, since gauge data was unavailable. Research shows that 1995 brought an extreme flood, which was predicted by the BWI. At this time over 100,000 ha of the Vientiane Plain was under more than a half-meter of water for up to 8 weeks. In human terms, the 1995 flood affected 153,398 people in the Vientiane Plain (out of a total population of 653,013 persons), 26,603 households, or 427 villages (FAO 1999). Importantly, we found that the BWI predictive model was robust, even when derived from the limited calibration period. Nonetheless, it captured this extreme event and its magnitude. Moreover, the BWI provided lead-time to the crest of the event, allowing a valuable opportunity to implement mitigation strategies. This result promotes confidence in applying the BWI to other basins where flow data is limited, which is a considerable number of the world's river.

3.3 River Basin Management: The Case of the Mekong

In locations where irrigation is a major component of agricultural production, economic planning around limited water resources is critical to the success of Climate Smart Agriculture. Specifically, it applies to allocation of river water to promote

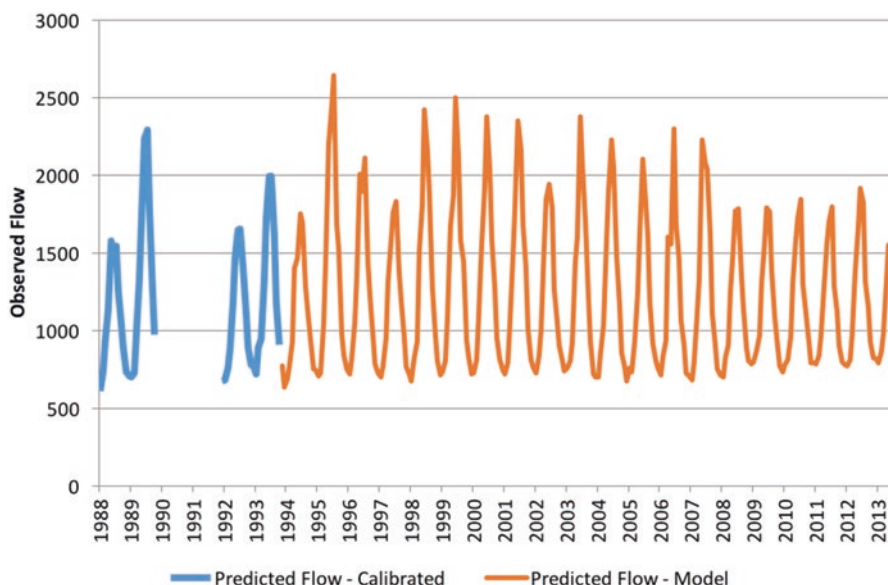


Fig. 11 The Mekong values of runoff (m^3/s per month, y-axis) and time (January 1988 through July 2013) display seasonality and the interannual variability over the calibration (predicted) in blue (red) period of the time series. Missing values are due to the lack of reliable SSM/I data

resilience to climate variability and optimize water allocation for economic growth. We provide a modified version of the empirical model used in Houba et al. (2013). The range of flow probabilities as measured by the BWI and at the gauging station Chiang Saen in Thailand are presented. These probabilities are used to calculate the expected value of basin benefits under various climatic scenarios. While the application of the BWI is demonstrated with the Mekong River Basin, we argue that it is a very simple process to apply the BWI to assist policy guidance in any of the river basins around the world, due to the fact that the main information needed for the analysis comes from satellite-based data, which is readily available. This application can benefit river basin planning, economic opportunities, resource management, and agricultural resilience.

3.3.1 Description of the Model

The model is based on a simplified hydrological structure of the basin, where water flows from China, hereafter noted as the Upper Mekong Basin (UMB) to the Lower Mekong Basin (LMB) and its tributaries, which originate in Thailand, Laos, Cambodia, and Vietnam, before the river enters the Delta (estuary), as seen in Fig. 12.

Basin-wide water availability is determined by water arriving from the UMB, and precipitation received in tributaries of the LMB. Water uses are aggregated in each sub region of the model into (1) industry and households, (2) hydropower

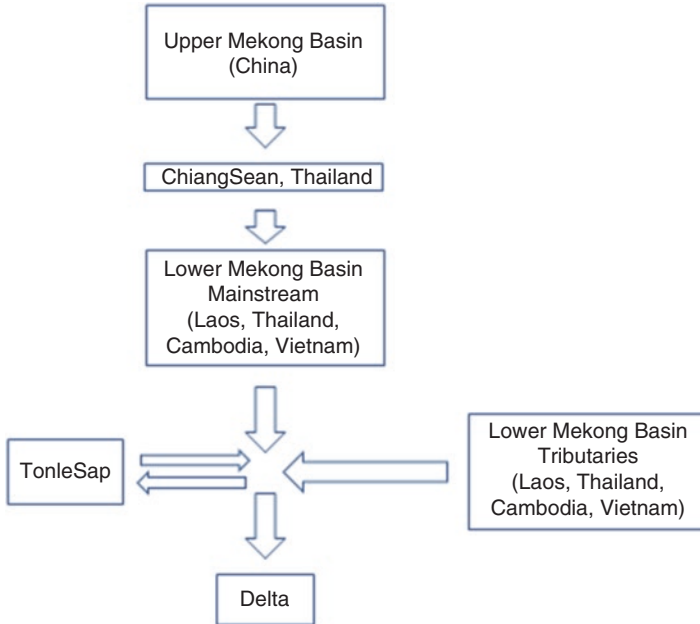


Fig. 12 Simple representation of the Mekong river basin used in our model (Modified from Houba et al. 2013). Note: We exclude Burma (Myanmar) from the analysis because it has a negligible share of water and land in the basin

generation, (3) irrigated agriculture, and (4) fisheries (Table 4). Water quality is measured in terms of salinity in Houba et al. (2013). In this paper we assume that salinity impacts fishery and irrigated agriculture. Hydropower generation is considered to be an in-flow user, while providing economic opportunities and growth. Moreover, water entering the first reservoir of a cascade can be reused and stored, over time, in all downstream reservoirs, which expanding capacity for economic growth along the river.

The model is calibrated on flow data from 2010 and it is static with an annual setup, represented by two seasons’ dynamics (wet and dry) across the entire basin. All modifications introduced in this paper comply with the original calibration. The water inflow for the mainstream of the LMB consists solely of the outflow received from China. Reservoirs/dams are filled in the wet season and the water is used during the dry season mainly for irrigation. During the wet season the Mekong water in UMB (China) can be used for industrial and household activities, fish production, storage for use in the dry season, and non-consumptive hydropower generation. Moreover, the wet season water supplies dry season irrigation for Climate Smart Agriculture. Moreover, effectively monitored outflow from mainstream UMB and tributary dams can promote inundations of wetlands in the delta. This nurtures fisheries production and flushes salinity from the estuary (Delta), which improves water quality and irrigation supplies.

Table 4 Water balances and use by sectors (km³/year) for mean flows at UMB and LMB tributaries

Variable	UMB wet season	UMB dry season	LMB wet season	LMB dry season
Inflow water	66.737	9.534	375.920	53.703
River flow from upstream			60.522	7.151
Water availability	66.737	9.534	436.442	60.854
Stored water total ^a	5.474		12.888	
H&I water use	0.741	0.529	1.895	1.352
Outflow water from dams	60.522	13.565	421.659	69.735
Irrigation		6.414		6.579
River flow to Tonle Sap			86.950	−86.950
River flow to downstream/estuaries	60.522	7.151	334.709	150.107
Hydropower water total ^b	69.226	74.912	60.003	42.860

Source: Houba et al. (2013)

^aWater is stored on main river in UMB and on tributaries in LMB

^bHydropower is produced on main river in UMB and on tributaries in LMB

Following Houba et al. (2013) the benefit, cost and loss functions in the model are quadratic, with the benefit function being concave (same as the flow parameters in the BWI model) and the cost and loss functions being convex to the origin. The volume of water that enters the Tonle Sap and then flows out into the Delta wetlands is a linear function of the river flow. Benefit functions were used for industry and households, hydropower generation, irrigated agriculture, and fisheries. The value function of the Tonle Sap and Delta/Wetlands assumes that all fishery production concentrates in that lake and surrounding wetlands. Salinity losses are modeled only in the LMB agricultural sector.

3.3.2 Applying the BWI to the Mekong Economic Model

A regression equation calibrates the BWI on gauge data from the UMB at Chiang Saen. The upper and lower basins have appreciably different geographies, sizes, and rainfall. Nonetheless, we applied the upstream hydrological model to the lower basin. Our assumption in doing so is that the BWI signal is designed to detect liquid water from all sources, and is defined as the percentage of the surface that is liquid water near the surface. Therefore, we explore the robustness of the model to detect that amount of water moving through the lower basin. Our hypothesis is that BWI values are a robust signal and the model parameters could effectively transcend different geographies.

There was the possibility of shifting the intercept, since the lower basin is appreciably larger, and therefore its base flow should be higher. However, we wanted to minimize any tuning, in order to test the robustness of the model. The only change is the lag was reduced from 2 to 1 month, to allow for better integration (time to

flow) from the upper basin into the lower basin. This, in turn, would allow us to model the flow as one kinematic wave based on the speed of flow.

In order to calculate the magnitude of water moving through the entire basin, the upper and lower basins were weighed in terms of their area (the large lower basin is a much larger area, and therefore has higher weights). This allowed us to integrate the upper and lower basins into one combined flow. Since the upper basin has a two-month lag, the first 2 months of 1988 and 1992 were set to be missing. A simple interpolation technique could easily and effectively be applied, since the beginning of the year is not a critical period of flow, however we did not apply it in order to minimize assumptions.

The average flow was derived from the BWI values and the model parameters over the period of record, in terms of cubic meters/second. To keep our economic optimization comparable with previous work Houba et al. 2013, we express water in cubic kilometers per year rather than in cubic meters per second ($1 \text{ m}^3/\text{s} = 0.031556926 \text{ km}^3/\text{year}$). The mean annual flow over the period of record derived by the BWI for the UMB and LMB is 424 km^3 , which is reasonably close to the independent assessments of annual mean flow on the Mekong, which range from 410 (Houba et al. 2013) to 475 (Mekong Water Commission 2009).

We were very encouraged by the fact that the flow numbers derived through the BWI wetness values were congruent with the expected flow values. Equally important, the monitored variation of flow from month to month, and year to year was accurately captured by the BWI values. For example, the major flood of 1995 and smaller flood of 2000 was also predicted by the BWI, providing a one-month lead-time to the magnitude of the flood, allowing time to mitigate its consequences.

We performed a similar analysis using precipitation inputs to predict mean annual flow for the Mekong. Specifically, we used the flow model parameters derived from the upper basin and applied them to the LMB, in order to determine integrated flow for the River as a whole. The calculated flow based on rainfall is 359, while the BWI provided a value of $424 \text{ km}^3/\text{year}$ (i.e. the BWI value is much closer to the consensus of the mean annual flow). This result was surprising; since the precipitation model had a slightly better explanatory power of flow in the upper basin, see Blankespoor et al. 2012. We interpreted this finding as demonstrating the robustness of the wetness index, and the ability to apply the model in areas outside of the region where they are calibrated. Consequently, we use the BWI flow predictions to enhance CSA, climate resilience, and calculate return periods of extreme events (Table 5).

3.3.3 Results of the Economic Model

We ran four scenarios, following the pairs $(a_i; b_i, i = 1, \dots, 4)$ of flow values from Table 5, which correspond to distribution of the flow in both the UMB and the LMB tributaries. As can be seen from Table 5, the distribution of the LMB tributaries flow is much more skewed towards lower values (drought) than the flow of the UMB. Table 6 presents the net welfare in each region for various distributions of the flow as obtained from the basin optimization model we run.

Table 5 Flow data in the UMB and LMB as calculated by the BWI

Description	km ³ /year	m ³ /sec	Cumulative probability	Probability
a. Flow at Chiang Saen (UMB coming from China)				
a1: Mean – 1 SD	27.863	882	0.117	0.117
a2: Mean	76.271	2416	0.588	0.471
a3: Mean + 1 SD	124.679	3950	0.862	0.274
a4: Mean + 2 SDs	173.087	5484	0.961	0.099
b. Flow of LMB tributaries				
b1: Mean – 1 SD	345.536	10,949	0.414	0.414
b2: Mean	429.623	13,614	0.576	0.162
b3: Mean + 1 SD	513.710	16,278	0.710	0.134
b4: Mean + 2 SD	597.797	18,943	0.809	0.099

Table 6 Net benefit calculations for various flow values in the Mekong basin (billion \$)

	Mean flow – 1 SD		Mean flow		Mean flow +1 SD		Mean flow +2 SD	
	UMB	LMB	UMB	LMB	UMB	LMB	UMB	LMB
km ³ /year	27.863	345.536	76.271	429.623	124.679	513.710	173.087	597.797
Net welfare created	2.376	3.222	2.656	6.663	2.544	6.445	2.313	6.336
Aggregated economic value	2.376	6.355	2.656	6.663	2.544	6.445	2.313	6.336
Econ value households and industry	0.408	1.957	0.408	1.957	0.408	1.957	0.408	1.957
Econ value fishery	0.128	2.772	0.241	2.728	0.167	2.077	0.082	1.109
Econ value irrigation	1.193	1.421	1.193	1.772	1.193	2.206	1.193	3.065
Econ value of hydro in main	0.647		0.815		0.776		0.629	
Econ value of hydro in tributaries		0.205		0.206		0.206		0.206
Aggregated economic costs		3.133		0.000				
Costs saltwater intrusion		3.133		0.000				

Source: Authors’ calculations

Note: *SD* standard deviation, *UMB* upper Mekong basin, *LMB* lower Mekong basin

As is apparent from Table 6, the net welfare generated in the UMB is \$2.656 billion and that of the LMB is \$6.663 billion, annually. Of the net welfare produced annually in the UMB, hydropower comprises 31%, irrigation 45%, fisheries 9% and households and industry 15%. For the LMB the values are 3%, 27%, 41%, and 30%, respectively. Table 6 also suggests that the damage from salinity due to seawater intrusion in the LMB is 0 for mean flow or above mean flow runs. However, losses of \$3.133 billion are encountered in the LMB in the case of the below mean flow run. It appears that the LMB is much more sensitive to flow fluctuations than the UMB. This is also apparent from Fig. 13, which summarizes the results in aggregate terms for different flow distributions by the Mekong regions. Both high and low levels of flow have a negative impact on net welfare of the basin.

Using the probabilities in Table 5 and the net benefits in Fig. 13 the expected total basin net benefit value at \$6.359 billion at one standard deviation below mean flow. This figure represents only 68% of the basin-wide net benefits (\$9.313 billion) that was estimated under the mean flow. Having the flow distribution information (as provided by the BWI) allows the basin riparians to reconsider arrangements that will secure their economies rather than face significant losses under extreme flow situations. Having probabilities assigned to the various flow values allows a cost-benefit analysis by policy makers who consider their interventions. The information can be used directly in Climate Smart Agriculture to promote cooperation for efficient and equitable water use in agriculture, as well as serve as a quantitative measure to implement early warning strategies to mitigate the losses from limited water supplies.

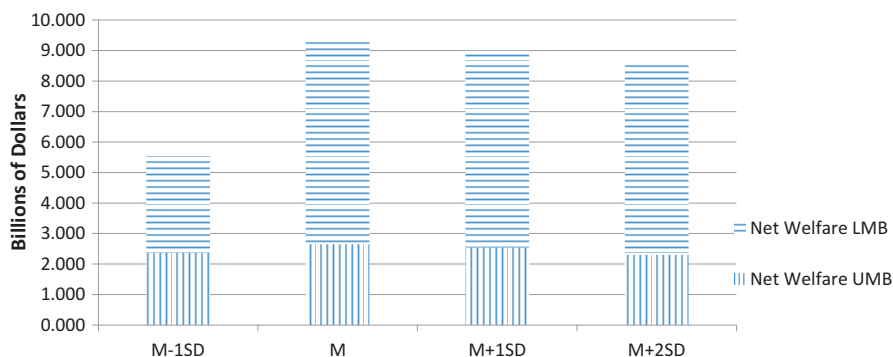


Fig. 13 Net benefits in the Mekong basin as a function of flow distribution. *M* mean, *SD* standard deviation

4 Concluding Discussion

This chapter demonstrates several applications of the satellite derived surface wetness and temperature data to promote CSA. First, the early detection of growing conditions and predicting the availability of food directly improves climate resilience and food security. Second, insurance (risk management) programs can use the indexes in triggers for a quick release of catastrophic bonds to farmers adversely impacted by the weather in order to mitigate the impact of crop failure. Third, these tools provide information to educate farmers about the viable yields from various crops under current and changing climatic conditions. Fourth, an early warning system distributed across the globe can help identify and expedite the exportation of food supplies from areas where they are in excess into areas where a deficiency is likely to occur.

The BWI has skill to predict river flows in several geographies and locations around the world, where it captured the integration of rainfall, melting snow cover, the change in wetland areas in a quantitative measure of river flow. It also provides a quantitative measurement that is independent of local governmental reports. We realize that more sophisticated models can generate more accurate calculations of flow. However these models require detailed parameterizations and assumptions, which means they are difficult to run and maintain, and they must be trained for each basin. Whereas the approach taken in this study is a simple, yet robust variable that has expanded application and portability to other basins and periods of time beyond the calibration time and location. This expands the accuracy and utility of the product for CSA.

In terms of adding new variables to interact with the wetness and temperature products, the Normalized Difference Vegetative index (NDVI) is a natural complement, since it is a direct measurement of canopy greenness. The three products together can be used as a superior signal of crop conditions and potential yields. The CSA will benefit directly by improving near real time monitoring capacity. In this situation the synergy between the three observations can create a superior tool for crop yield predictions, insurance triggers, trends and return period of extreme events, all of which improve climate resilience.

In order to maximize the skill of crop prediction models, it is essential to calibrate the models with reliable yield data from at least 10 years and preferably 20–25 years. Most countries collect field data and calculate yields, however the spatial resolutions of the values can range from county (districts) to province (states, oblast), all the way to country-wide estimates. Since these yield values are always best guesses, CSA needs independent, objective and transparent tools to assess the food production at the regional level in across the globe in near real time. This is a particularly important requirement, since many countries do not release their best estimates; instead the data they do release is manipulated data for national security, political and economic reasons. Consequently, models based on these yield data lack both skill and confidence in their predictions. One approach is to use analogues from areas that grow the same crop and share similar climate, soils, and irrigation practices. In this case, the models developed in the analogue region can be applied to the target area.

Another application to the CSA is using the indexes and predictions as triggers to release catastrophic bonds to farmers having substantial crop failure. There are several advantages to index-based insurance that support CSA.

1. The cost of the premium is substantially lower than the traditional indemnification insurance programs, since no adjuster or field survey are required.
2. The funds are released in near real time, mitigate the impact of the financial losses of the harvest.
3. It is an objective program that can be readily underwritten by numerous sources, thereby the distribution of the losses through various government and financial institutions, reducing exposure to a particular organization. Insurance based on a composite of indexes (used as triggers) has been tried with some success. However, one of the major obstacles is confidence in the triggers by both the insurance companies and the farmers. One intention of the study is to support the CSA's ability to identify reliable and easy to apply triggers in the crop insurance industry.

The value of the wetness index for monitoring and predicting river flow is multifold.

1. Improved knowledge on the distribution of water resources and the probability of various levels of water for agriculture, commercial, industrial and human consumption is critical to sustainability and development strategies.
2. Mitigate the impact of flood and drought with a reliable early warning system, which provides valuable lead-time about upcoming extreme events.
3. Provide a reliable and objective source of information about the available water resources, in planning and promoting water sharing between riparian states .
4. Use objective measurements to establish an insurance program that protects sectors of society against extreme events, and provides financial compensations for mitigating impacts on infrastructure and society's welfare.

We introduced a model to demonstrate how to quantify the value on water resources in various sectors of society. The model broke the impacts across the agriculture, fishing, commercial and human consumption. There are many benefits to use the BWI to quantify these relationships, in terms of social and economic costs/benefits related to water resource management and mitigation strategies against extreme events. This chapter demonstrates the application of both the wetness and temperature data for monitoring growing conditions and predicting yields, which directly support CSA around the world. We plan to integrate these products with various datasets, such as in situ surface temperature, the greenness index, and soil moisture data, in order to expand their complementary value and utility. We are excited about collaborating with organizations that would like to apply these products in various sectors. Since the data is global and has more than 25 years of observations, we believe that the potential for application is vast and look forward to developing that potential in many areas. The goal is to assist the CSA by applying these products to support resource management, food security, climate resilience, as well as mitigate the adverse impacts of extreme events.

References

- Adger, N., T. Hughes, C. Folke, S. Carpenter, and J. Rockström (2005), Social ecological resilience to coastal disasters. *Science*, 309, 5737, 1036–1039.
- Ambec, S., A. Dinar, and D. McKinney (2013), Water sharing agreements sustainable to reduced flows, *Journal of Environmental Economics and Management*, 66(3), 639–655.
- Basist, A., Grody, N. C., Peterson, T. C., and Williams, C. N. (1998), “Using the Special Sensor Microwave / Imager to Monitor Land Surface Temperatures, Wetness, and Snow Cover,” *Journal of Applied Meteorology*, 37(September): 888–911.
- Basist, A., C. Williams Jr, T. F. Ross, M. J. Menne, N. Grody, R. Ferraro, S. Shen, and A. T. C. Chang (2001), Using the Special Sensor Microwave Imager to monitor surface wetness, *Journal of Hydrometeorology*, 2(3), 297–308.
- Becker-Reshef I, Vermote E, Lindeman M, Justice C (2010) A generalized regression-based model for forecasting winter wheat yields in Kansas and Ukraine using MODIS data. *Remote Sensing of Environment* 114: 1312–1323
- Blankespoor, B., A. Basist, A. Dinar and S. Dinar (2012), Assessing Economic and Political Impacts of Hydrological Variability on Treaties: Case Studies of the Zambezi and Mekong Basins Policy Research Working Paper No. 5996, 1–56 pp, World Bank, Washington, DC.
- Demirel Mehmet C., Martijn J. Booij and Arjen Y. Hoekstra (2013) Identification of appropriate lags and temporal resolutions for low flow indicators in the River Rhine to forecast low flows with different lead times *Hydrological Processes*. 27(19): 2742–2758,
- Deryng, D., W. J. Sacks, C. C. Barford, and N. Ramankutty, 2011: Simulating the effects of climate and agricultural management practices on global crop yield. *GLOBAL BIOGEOCHEMICAL CYCLES*, VOL. 25, GB2006, 1–18.
- Dinar, A., B. Blankespoor, S. Dinar, and P. Kurukulasuriya (2010), Does precipitation and runoff variability affect treaty cooperation between states sharing international bilateral rivers?, *Ecological Economics*, 69(12), 2568–2581.
- Dinar, S., D. Katz, L. De Stefano, and B. Blankespoor (2015), Climate Change, Conflict, and Cooperation: Global Analysis of the Effectiveness of International River Treaties in Addressing Water Variability. *Political Geography*.
- Drieschova, A., M. Giordano and I. Fischhendler (2008), Governance mechanisms to address flow variability in water treaties. *Global Environmental Change*, 18, 285–295.
- Drury, A. C., and R. S. Olson (1998), Disasters and Political Unrest: An Empirical Investigation, *Journal of Contingencies & Crisis Management*, 6(3), 153.
- (FAO) Food and Agricultural Organization of the United Nations, Mekong River Commission Secretariat and Department of Irrigation, Ministry of Agriculture and Forestry of LAO P.D.R. (1999), Flood Management and Mitigation in the Mekong River Basin, 40pp, FAO, Bangkok. Accessed 2014–10 at: <http://www.fao.org/3/a-ac146e/AC146E01.htm>
- Gutman, Nsthanil B. 1999: Accepting the standardized precipitation index: A Calculation algorithm, *Journal of the American water resources association*. Vol. 35, No.2, 311–322.
- Hendrix, C. S., and I. Salehyan (2012), Climate change, rainfall, and social conflict in Africa, *Journal of Peace Research*, 49(1), 35–50.
- Houba, H., Kim Hang Pham Do, and X. Zhu (2013), Saving a river: a joint management approach to the Mekong River Basin, *Environment and Development Economics*, 18:93–109.
- Intelligence Community Assessment (2012), Global water security. Office of the Director of National Intelligence, February 2.
- Jackson, T. Passive microwave remote sensing of soil moisture and regional drought monitoring, (2005). V:89–104. in Boken, V. (ed.) *Monitoring and Predicting Agricultural Drought*. Oxford Univ. Press
- Jury, W. A., and H. Vaux (2005), The role of science in solving the world’s emerging water problems, *Proceedings of the National Academy of Sciences of the United States of America*, 102(44), 15715–15720.

- Larson, D. F., A. Dinar, and B. Blankespoor (2015), Aligning Climate Change Mitigation and Agricultural Policies in ECA, in *Asia and the World Economy*, edited by J. Whalley, pp. 69–151, World Scientific, Singapore.
- Mekong Water Commission (2009), Annual Report. <http://mwcmekong.org>.
- Miller, K., and D. Yates (2006), *Climate change and water resources: a primer for municipal water providers*, 83 pp., American Water Works Research Foundation and UCAR, Denver, CO.
- NASA (2010), Flooding on the Zambezi River: Natural Hazards, edited, NASA, <http://earthobservatory.nasa.gov/IOTD/view.php?id=44132>.
- Nel, P., and M. Righarts (2008), Natural Disasters and the Risk of Violent Civil Conflict, *International Studies Quarterly*, 52(1), 159–185.
- Palmer, M. A., C. A. Reidy Liermann, C. Nilsson, M. Flörke, J. Alcamo, P. S. Lake, and N. Bond (2008), Climate change and the world's river basins: anticipating management options, *Frontiers in Ecology and the Environment*, 6(2), 81–89.
- Tucker, C.J., M. E. Brown, J. E. Pinzon, D. A. Slayback, R. Mahoney, N. E. Saleous, and E. F. Vermote: 2005, "An extended AVHRR 8-km NDVI dataset comparable with MODIS and SPOT Vegetation NDVI data," *Int. J. Remote Sens.* 26:4485–4498.
- Williams, C., A. Basist, T. C. Peterson, and N. Grody 2000: Calibration and Verification of Land Surface Temperature Anomalies Derived from the SSMI, *Bull. Of the Amer. Meteor. Soc.* 2141–2156.
- Winsemius, H. C., H. H. G. Savenije, A. M. J. Gerrits, E. A. Zapreeva, and R. Klees (2006), Comparison of two model approaches in the Zambezi river basin with regard to model reliability and identifiability, *Hydrol. Earth Syst. Sci.*, 10, 339–352.

Open Access This chapter is distributed under the terms of the Creative Commons Attribution-NonCommercial-ShareAlike 3.0 IGO license (<https://creativecommons.org/licenses/by-nc-sa/3.0/igo/>), which permits any noncommercial use, duplication, adaptation, distribution, and reproduction in any medium or format, as long as you give appropriate credit to the Food and Agriculture Organization of the United Nations (FAO), provide a link to the Creative Commons license and indicate if changes were made. If you remix, transform, or build upon this book or a part thereof, you must distribute your contributions under the same license as the original. Any dispute related to the use of the works of the FAO that cannot be settled amicably shall be submitted to arbitration pursuant to the UNCITRAL rules. The use of the FAO's name for any purpose other than for attribution, and the use of the FAO's logo, shall be subject to a separate written license agreement between the FAO and the user and is not authorized as part of this CC-IGO license. Note that the link provided above includes additional terms and conditions of the license.

The images or other third party material in this chapter are included in the chapter's Creative Commons license, unless indicated otherwise in a credit line to the material. If material is not included in the chapter's Creative Commons license and your intended use is not permitted by statutory regulation or exceeds the permitted use, you will need to obtain permission directly from the copyright holder.

